Endogenous Piezo1 Can Confound Mechanically Activated Channel Identification and Characterization

Adrienne E. Dubin, Swetha Murthy, Amanda H. Lewis, Lucie Brosse, Stuart M. Cahalan, Jorg Grandl, Bertrand Coste, Ardem Patapoutian

Endogenous Piezo1 Can Confound Mechanically Activated Channel Identification and Characterization

Adrienne E. Dubin, Swetha Murthy, Stuart M. Cahalan, Amanda H. Lewis, Lucie Brosse, Jorg Grandl, Bertrand Coste, Ardem Patapoutian

Endogenous Piezo1 can confound mechanically-activated channel identification and characterization

Adrienne E. Dubin[1,#], **Swetha Murthy**[1,#], **Amanda H. Lewis**[2], **Lucie Brosse**[3], **Stuart M. Cahalan**[1,^], **Jörg Grandl**[2], **Bertrand Coste**[3], and **Ardem Patapoutian**[1,*]

[1]Howard Hughes Medical Institute, Department of Neuroscience, Dorris Neuroscience Center, The Scripps Research Institute, La Jolla, California 92037, USA

[2]Department of Neurobiology, Duke University School of Medicine, 311 Research Drive, Box 3209, Durham, North Carolina 27710, USA

[3]Aix Marseille Universite, CNRS, CRN2M, Marseille, France

Summary

A gold standard for characterizing mechanically-activated (MA) currents is via heterologous expression of candidate channels in naïve cells. Two recent studies described MA channels using this paradigm. TMEM150c was proposed to be a component of a MA channel partly based on a heterologous expression approach (Hong et al., 2016). In another study, Piezo1's N-terminal “propeller” domain was proposed to constitute an intrinsic mechanosensitive module based on expression of a chimera between a poreforming domain of the mechano-insensitive ASIC1 channel and Piezo1 (Zhao et al., 2016). When we attempted to replicate these results we found each construct conferred modest MA currents in a small fraction of naïve HEK cells similar to the published work. Strikingly, these MA currents were not detected in cells in which endogenous Piezo1 was CRISPR/Cas9-inactivated. These results highlight the importance of choosing cells lacking endogenous MA channels to assay the mechanotransduction properties of various proteins. This Matters Arising paper is in response to Hong et al. (2016) and Zhao et al. (2016) in Neuron. See also the response papers by Hong et al. and Zhao et al., published concurrently with this Matters Arising.

Introduction

Mechanically activated (MA) ion channels are sensors that are critical for hearing, touch, pain, and regulating blood pressure (Ranade et al., 2015). The MA channels Piezo and NOMPC are sufficient to induce MA currents when transfected in naïve cells such as

[*]Corresponding Author and Lead Contact, ardem@scripps.edu.
[#]These authors contributed equally
[^]Current address: Vertex Pharmaceuticals Inc., 11010 Torreyana Rd, San Diego, CA 92121, USA

Author Contributions. AED, SM, AHL, LB, and SMC conducted the experiments, JG, BC and AP designed the experiments and JG, BC, AED and AP wrote the paper.

HEK293 (HEK) and S2 cells (Coste et al., 2010; Yan et al., 2013). Fulfilling this requirement for sufficiency is critical for identifying novel MA ion channels and making conclusions in biophysical studies on mutated MA channels. Two recent reports claim that heterologous expression of particular constructs in HEK cells was sufficient to mediate MA currents dependent on the exogenous protein. In one, Tentonin 3 (TTN3)/TMEM150c was proposed to be a component of a MA channel based on several experiments, including the finding that heterologous expression of TMEM150c in HEK cells gives rise to MA currents (Hong et al., 2016). In the other, a chimera (mPiezo1(1-2190)-mASIC1, "Piezo1-ASIC1") which combined the large N-terminal "propeller" domain of Piezo1 that lacks the pore (Coste et al., 2015; Ge et al., 2015; Zhao et al., 2016) with the pore-forming domain of the mechanically-insensitive, sodium-selective ASIC1 was reported to give rise to MA currents when transfected in HEK cells (Zhao et al., 2016). Based on this result, the authors concluded that the N-terminal portion of Piezo1 constitutes an intrinsic mechanosensitive module (Zhao et al., 2016). In both studies, the fraction of HEK cells responding to membrane displacement using a piezo-electrically driven glass probe was only half of those tested and whole-cell current amplitudes were on average sub-nanoampere (nA). Since HEK cells express low levels of Piezo1 mRNA, and small detectable MA currents have been observed in these cells (Bae et al., 2013; Lukacs et al., 2015), we sought to verify that currents observed in cells transfected with either TMEM150c or Piezo1-ASIC1 were mediated by the exogenously expressed construct and not by endogenous Piezo1.

Results and Discussion

We used a blunt glass pipette to assess mechanical responses in naïve HEK cells *in vitro*. Mechanical stimulation induced small, slowly inactivating MA currents at a holding potential of -80 mV in about half of the parent HEK cells transfected 1-3 days earlier with empty vector (Fig.1a open circles ("Vector"), Fig.1b **left**). The magnitude of these currents was stimulus-dependent and the apparent threshold (the distance between touching the cell and first detectable current) ranged from 5 μm to close to the cell diameter (Fig.1b **right**, black symbols). The inactivation kinetics of the currents observed in vector-transfected cells were slow, and do not resemble those observed when Piezo1 is overexpressed in HEK cells (Fig.1c **left**)(Bae et al., 2011; Coste et al., 2010). However, slower inactivation kinetics of Piezo1-dependent currents in other cell types has been observed in cell-attached recordings (Bae et al., 2015; Lee et al., 2014; Pathak et al., 2014; Peyronnet et al., 2013; Servin-Vences et al., 2017). We previously created a more reliable mechanically silent cell line for expression studies by inactivating endogenous Piezo1 in HEK cells (HEK-P1KO) using CRISPR/Cas9 to truncate all Piezo1 alleles (Lukacs et al., 2015). These cells propagate similarly to naïve HEK cells. As described previously, no MA currents were detected in cells lacking Piezo1 (Fig.1a red open circles, Fig.1b **middle and right**, red) (see Methods for information on HEK-P1KO genotype). These data confirm that all endogenous MA currents observed in naïve HEK cells are Piezo1-dependent.

To ensure that HEK-P1KO cells are not compromised in their ability to express MA channels, we tested whether exogenous Piezo1 expression gives rise to typical MA currents compared to those in parent HEK cells. Large whole-cell Piezo1 currents were observed in HEK-P1KO cells transfected with exogenous Piezo1 (Fig.1a **right**; Fig.1c **middle, right** red

symbols). Maximum peak currents (I_{max}) were similar to those observed in HEK cells (Fig. 1c **left, right** black symbols). Characteristics of the exogenous Piezo1-mediated whole-cell currents were not different in the two cell lines; the inactivation time constant (tau) at -80 mV was 12.4 ± 1.7 ms (n=9) and 14.2 ± 1.8 ms (n=13) (P> 0.1; Student's *t*-test; mean ± sem), and the apparent threshold for activation was 5.8 ± 0.8 μm and 5.0 ± 0.8 μm (P>0.3) in HEK and HEK-P1KO, respectively. I_{max} was obtained at similar displacements above threshold for the 2 cell lines (4.1 ± 0.4 μm (n=9) and 4.5 ± 0.6 μm (n=13) for HEK and HEK-P1KO cells, respectively). Thus, we conclude that HEK-P1KO cells, similarly to parent HEK cells, are capable of expressing bona fide MA ion channels.

We next tested whether MA currents could be observed in HEK cells transfected with TMEM150c and Piezo1-ASIC1 constructs. About half the tested HEK cells transfected with either construct were responsive to membrane displacement (Fig.1a, black filled symbols; 16 of 31 (52%) and 16 of 34 (47%) of cells transfected with TMEM150c and Piezo1-ASIC1, respectively). Non-responsive TMEM150c- and Piezo1-ASIC1-transfected cells showed no MA currents up to displacements of 10.5 ± 0.8 μm (n=15) and 12.6 ± 0.6 μm (n=18) beyond visibly touching the cell, respectively. The observed I_{max} amplitudes at -80 mV ranged from about -15 to -1250 pA (TMEM150c) and -50 to -720 pA (Piezo1-ASIC1) (Fig.1a black symbols). Currents inactivated slowly (Fig1.d, e **left**), similar to those observed in vector control-transfected HEK cells (Fig.1b, **left**). Among the responding cells, more robust responses to mechanical stimuli were observed in cells expressing TMEM150c (P< 0.02; Student's *t*-test) and Piezo1-ASIC1 (P< 0.05) compared to vector-transfected HEK cells as previously reported (Hong et al., 2016; Zhao et al., 2016). It is also interesting that the apparent threshold for responsive vector-transfected HEK cells (12.4 ± 1.1 μm, n=11) was about twice that observed for cells expressing either TMEM150c or Piezo1-ASIC1. The I_{max} observed for these constructs, however, was significantly less than what was observed with the bona fide MA channel Piezo1 (P<0.005 in both cases, Fig. 1a, **right**). These results confirm the findings of the two previous reports (Hong et al., 2016; Zhao et al., 2016) of increased MA channel activity in HEK cells transfected with these putative mechanosensors.

We next tested whether TMEM150c- and Piezo1-ASIC1-induced MA currents were dependent on endogenous Piezo1 expression. HEK-P1KO cells were transfected with either TMEM150c or Piezo1-ASIC1 under conditions identical to HEK cells and tested at similar times after transfection in 3 or 5 separate experiments, respectively (Fig.1a,d,e, red traces and symbols). Representative MA current traces are shown for HEK-P1KO cells transfected with TMEM150c (Fig.1d, red) and Piezo1-ASIC1 (Fig.1e, red). None of 41 TMEM150c-transfected cells revealed any MA current, even with displacements three times greater than the average displacement required to elicit MA current in HEK cells expressing Piezo1 or TMEM150c (indicated by the circle above the displacement-response curve (Fig.1d **right**)). Only 1 of 29 Piezo1-ASIC1-transfected cells revealed an apparent response, but the cell was lost at the next stimulation and this may have been an artifact. We would normally not include this cell as a responder because our criteria for inclusion requires that cells show stimulus-dependent responses with no unusual off-responses, but we included it here because the single response had characteristics of a bona fide MA current. Thus, when HEK-P1KO cells were transfected with Piezo1-ASIC1 or TMEM150c, no reliable MA responses

were detected during displacements up to three times the average apparent threshold observed in HEK cells.

The experiments described above were performed in the Patapoutian laboratory. Similar experiments were performed separately in the laboratories of Drs. Bertrand Coste (Aix Marseille Universite) and Jörg Grandl (Duke University). Similarly, whole-cell MA currents were observed in naïve HEK cells transfected with TMEM150c and Piezo1-ASIC1, but not in HEK-P1KO cells (Fig.2 and Fig.3).

Our results indicate that using conventional HEK cells as a heterologous expression system for studying MA currents can be misleading due to endogenously expressed Piezo1 channels. Rather than recording MA currents directly mediated by TMEM150c or Piezo1-ASIC1constructs in HEK cells, these studies have instead identified conditions that enhance endogenous Piezo1 activity. Unraveling the molecular mechanisms of Piezo1 modulation by these proteins will provide insights into mechanotransduction. Indeed, it is not clear at this time why overexpression of TMEM150c or Piezo1-ASIC1 potentiates endogenous Piezo1 currents. It is possible that TMEM150c, for example, enhances Piezo channel activity and/or surface expression. It is also possible that transfection of Piezo1-ASIC1 causes unknown stresses to cells that indirectly modulate Piezo function. Regardless, our results demonstrate that the whole-cell currents observed in HEK cells transfected with TMEM150c and the Piezo1-ASIC1 chimera are dependent on the expression of endogenous Piezo1 in these cells. We are confident that Piezo1-deficient HEK cells are healthy and capable of sustaining MA channel function, as Piezo1 overexpression in naïve HEK and HEK-P1KO cells gave rise to MA currents that were indistinguishable from each other. Furthermore, both cell lines maintained good holding currents at strong stimuli just prior to “losing” the cell, and the strongest displacements achievable in our dataset were similar to, if not higher than, those reported previously (Hong et al., 2016; Zhao et al., 2016). As an alternative hypothesis, one could imagine that endogenous inactivated Piezo1 in HEK-P1KO cells, if present, is acting as a dominant negative to suppress Piezo1-ASIC1 activity. However, this seems implausible because dominant negative function depends on comparable stoichiometry, and the transfected construct (Piezo1-ASIC1) is expected to be logs in excess of any truncated endogenous Piezo1. Regardless, one other reason to suspect that Piezo1-ASIC1 is not directly responsible for the MA currents in HEK cells: the observed Piezo1-ASIC1 currents are nonselective cationic (Zhao et al., 2016) instead of the expected sodium-selective for ASIC1a channels (Gründer and Chen, 2010).

Overall, our results highlight the importance of using mechanically nonresponsive naïve cell lines to assess MA currents in heterologous systems. The presence of endogenous Piezo1 may confound some types of biophysical characterization (e.g., steady state inactivation) of overexpressed bona fide mechanically activated channels (Piezo1, Piezo2, NOMPC) in HEK293 cells as well as other cell lines. For most parameters, the contribution of endogenous Piezo1 is likely extremely low since nanoampere exogenous MA currents are at least an order of magnitude larger than endogenous high threshold Piezo1-mediated currents. When investigating Piezo-mediated steady state currents, most studies have used native cells or corroborated conclusions using native cells. Nevertheless, when only a fraction of

transfected naïve HEK293 cells show a particular response, it is reason to suspect a possible role of endogenous MA channels.

STAR Methods

Contact for Reagent and Resource Sharing

Further information and requests for resources and reagents should be directed to and will be fulfilled by the Lead Contact Ardem Patapoutian (ardem@scripps.edu).

Experimental Model and Subject Details

Cell Lines—HEK293T from two sources (ATCC Cat#CRL-3216 and DSMZ Cat#ACC-635). The HEK-P1KO lines described were created in house. All cells were maintained as indicated by the supplier : DMEM with high glucose, 10% heat inactivated FBS, and pen-strep.

Method Details

Cell culture and transfection—Both HEK293T ("HEK"; DSMZ Cat# ACC-635, RRID:CVCL_0063 and ATCC Cat# CRL-3216) and HEK-P1KO cell lines were maintained in DMEM (high glucose) with 10% FBS and pen/strep antibiotics. The HEK-P1KO cells required a longer time to recover after thawing (up to 4-5 passages) compared to HEK cells. Cells were plated on poly-D-lysine coated coverslips (TSRI, AMU) or poly-D-lysine and laminin (Duke University). The Piezo1 positive control used was hPiezo1-pIres2-EGFP (Lukacs et al., 2015) and negative control was the corresponding empty vector (pIres2-EGFP). Maxi-preps of the two constructs were fully sequence verified by all laboratories. The mP1-mASIC1-mRuby (C-terminal fusion) construct (gift from Dr. Bailong Xiao) was sequence-verified (the ASIC1 isoform is ASIC1a) and tested 1-2 days after transfection; TMEM150c-ires-AcGFP (gift from Dr. U. Oh) was sequence-verified and tested 2-3 days after transfection. Transfection protocol differed somewhat between laboratories: Lipofectamine 2000 (TSRI, AMU) or Fugene6 (Duke) was used to transfect cells according to the manufacturer's instructions. Cells were exposed to Lipofectamine 2000 during plating on coverslips. For Fugene transfections, cells in 6-well plates were transfected two days prior to recording and replated onto coverslips the day before.

Electrophysiology—Whole-cell recordings were performed at three separate locations using methods essentially as previously described (Coste et al., 2010; Coste et al., 2015; Dubin et al., 2012). Vector- and Piezo1-transfected cells were tested 1-3 days and 1-2 days after transfection, respectively. Mechanical stimulation was applied to cells using a fire-polished glass pipette (tip diameter ~5 μm) positioned at an angle of 70° with respect to the cell. Recording pipettes contained the CsCl-based intracellular solution described in Coste et al., 2010 with some exceptions. Mg-ATP was 2 or 4 mM and Na_2-GTP was 200 or 400 μM, to mimic conditions described in (Hong et al., 2016; Zhao et al., 2016). The intracellular solution used at Duke differed in that EGTA was 1 mM and no Ca^{2+} was added, $MgCl_2$ was 2 rather than 1 mM, and Na_2GTP was 300μM; the extracellular solution contained 5 instead of 10 mM glucose, and 5 mM TEA-Cl was added. Currents were sampled at 20 kHz (TSRI, AMU) or 10 kHz (Duke) and filtered at 2 kHz (TSRI, AMU) or 2.9 kHz (Duke); membrane

holding potential was -80 mV. A cell was considered a responder only if it showed a stimulus-dependent response with no unusual off-response (note: the single Piezo1-ASIC1 HEK-P1KO responder did not fit this criteria but we included it here as the only potential responder). In some cases the experimenter was blinded to the cell type (Duke). The sample size was based on the differences observed for whole cell currents observed 1-3 days after transfection of constructs in wild type HEK293T and HEK-P1KO cells.

Creation and genotyping of HEK-P1KO cell lines (HEK-P1KO cell line authentication)—Clonal HEK-P1KO cell lines were derived from HEK293T cells edited by CRISPR-Cas9 as described in Lukacs et al. (Lukacs et al., 2015). To verify the introduction of frameshift-causing mutations, the genomic region flanking the target sequence was determined by PCR using the primers hP1 Locus F: CCACGTGTAGGGTGACTGTT; hP1 Locus R: GCCTCGTGATCAGCTAGTGG. Phire II Polymerase (ThermoFisher) was used according to manufacturer's instructions with a 59 °C annealing temperature and 15 second extension time. The PCR products were directly sequenced using the hP1 Locus F and were also subcloned into EcoRV-digested pBluescript SK+, with a minimum of 12 colonies sequenced to identify the sequences of each Piezo1 locus.

The mutations of the clonal lines were as follows:

Clone 1C10 – Homozygous indel consisting of 426 nt deletion of chr16: 88,719,825-88,720,250 and 5 nt TACAA insertion at chr16: 88720250. This indel is expected to result in a Piezo1 protein sequence of K_{1984} - HSAATDITSSLYSTSSSSRGSGWCRSWWSCGQ*

Clone 5E3 – Heterozygous mutations consisting of: Allele 1 – 2 nt deletion of chr16:88,720,247-88,720,248; Allele 2 – 1 nt A insertion at chr16:88,720,248. These mutations are expected to result in Piezo1 protein sequences of: Allele 1 - K_{1984} - HSAATDITSSLRRPGTRGFPGHAADPVQYHGG*; Allele 2 - K_{1984} - HSAATDITSSLIRRPGTRGFPGHAADPVQYHGG*

qPCR analysis was not performed for Piezo1 as the extremely low endogenous expression precludes accurate determination. Both clones 1C10 and 5E3 showed identical results by electrophysiology.

Quantification and Statistical Analysis

Student's t-test was used to determine significance (Fig.1). Mean ± sem is indicated in all cases for the indicated n which represents individual cells tested for each condition shown. For panel **c (right)** the circles above the axis represent n=9 and 13 for HEK (black) and HEK-P1KO (red); for panel **d (right)**, n=16 for HEK; for panel **e (right)**, n=16 for HEK. Whole cell currents were analyzed using pCLAMP10 software (Clampfit) and data were analyzed and presented using GraphPad Prism6 and Adobe Illustrator CS6. D'Agostino & Pearson omnibus normality test was used to determine whether the data subjected to the Student's *t*-test (Fig. 1) are distributed according to a Gaussian curve; each data set passed (Prism6).

Acknowledgments

We thank Maria Florendo and Tess Whitwam for help with preparing and verifying cDNA constructs, and Dr. Kara Marshall for her careful reading of the manuscript and valuable comments. We are grateful to Drs. Bailong Xiao and Uhtaek Oh for providing the mP1-mASIC1-mRuby (C-terminal fusion) and TMEM150c-ires-AcGFP constructs, respectively. The authors declare no competing interests.

This work was supported by grants from the National Institutes of Health grant R01NS083174 awarded to A.P., R21DE025329 awarded to A.E.D., F32NS094088 awarded to A.L, and funding from the European Research Council/ERC Grant Agreement n. 678610 to L.B. and B.C. A.P. is an investigator of the Howard Hughes Medical Institute.

References

Bae C, Gnanasambandam R, Nicolai C, Sachs F, Gottlieb PA. Xerocytosis is caused by mutations that alter the kinetics of the mechanosensitive channel PIEZO1. Proceedings of the National Academy of Sciences. 2013; 110:E1162–E1168.

Bae C, Sachs F, Gottlieb PA. The Mechanosensitive Ion Channel Piezo1 Is Inhibited by the Peptide GsMTx4. Biochemistry. 2011; 50:6295–6300. [PubMed: 21696149]

Bae C, Sachs F, Gottlieb PA. Protonation of Human PIEZO1 Ion Channel Stabilizes Inactivation. Journal of Biological Chemistry. 2015; 290:5167–5173. [PubMed: 25561736]

Coste B, Mathur J, Schmidt M, Earley TJ, Ranade S, Petrus MJ, Dubin AE, Patapoutian A. Piezo1 and Piezo2 Are Essential Components of Distinct Mechanically Activated Cation Channels. Science. 2010; 330:55–60. [PubMed: 20813920]

Coste B, Murthy SE, Mathur J, Schmidt M, Mechioukhi Y, Delmas P, Patapoutian A. Piezo1 ion channel pore properties are dictated by C-terminal region. Nat Commun. 2015; 6:7223–7233. [PubMed: 26008989]

Dubin, Adrienne E., Schmidt, M., Mathur, J., Petrus, Matthew J., Xiao, B., Coste, B., Patapoutian, A. Inflammatory Signals Enhance Piezo2-Mediated Mechanosensitive Currents. Cell Reports. 2012; 2:511–517. [PubMed: 22921401]

Ge J, Li W, Zhao Q, Li N, Chen M, Zhi P, Li R, Gao N, Xiao B, Yang M. Architecture of the mammalian mechanosensitive Piezo1 channel. Nature. 2015; 527:64–69. [PubMed: 26390154]

Gründer S, Chen X. Structure, function, and pharmacology of acid-sensing ion channels (ASICs): focus on ASIC1a. International Journal of Physiology, Pathophysiology and Pharmacology. 2010; 2:73–94.

Hong GS, Lee B, Wee J, Chun H, Kim H, Jung J, Cha Joo Y, Riew TR, Kim Gyu H, Kim IB, et al. Tentonin 3/TMEM150c Confers Distinct Mechanosensitive Currents in Dorsal-Root Ganglion Neurons with Proprioceptive Function. Neuron. 2016; 91:107–118. [PubMed: 27321926]

Lee W, Leddy HA, Chen Y, Lee SH, Zelenski NA, McNulty AL, Wu J, Beicker KN, Coles J, Zauscher S, et al. Synergy between Piezo1 and Piezo2 channels confers high-strain mechanosensitivity to articular cartilage. Proceedings of the National Academy of Sciences. 2014; 111:E5114–E5122.

Lukacs V, Mathur J, Mao R, Bayrak-Toydemir P, Procter M, Cahalan SM, Kim HJ, Bandell M, Longo N, Day RW, et al. Impaired PIEZO1 function in patients with a novel autosomal recessive congenital lymphatic dysplasia. Nat Commun. 2015; 6:8329–8335. [PubMed: 26387913]

Pathak MM, Nourse JL, Tran T, Hwe J, Arulmoli J, Le DTT, Bernardis E, Flanagan LA, Tombola F. Stretch-activated ion channel Piezo1 directs lineage choice in human neural stem cells. Proceedings of the National Academy of Sciences. 2014; 111:16148–16153.

Peyronnet R, Martins JR, Duprat F, Demolombe S, Arhatte M, Jodar M, Tauc M, Duranton C, Paulais M, Teulon J, et al. Piezo1-dependent stretch-activated channels are inhibited by Polycystin-2 in renal tubular epithelial cells. EMBO Rep. 2013; 14:1143–1148. [PubMed: 24157948]

Ranade, Sanjeev S., Syeda, R., Patapoutian, A. Mechanically Activated Ion Channels. Neuron. 2015; 87:1162–1179. [PubMed: 26402601]

Servin-Vences MR, Moroni M, Lewin GR, Poole K. Direct measurement of TRPV4 and PIEZO1 activity reveals multiple mechanotransduction pathways in chondrocytes. eLife. 2017; 6:e21074. [PubMed: 28135189]

Yan Z, Zhang W, He Y, Gorczyca D, Xiang Y, Cheng LE, Meltzer S, Jan LY, Jan YN. Drosophila NOMPC is a mechanotransduction channel subunit for gentle-touch sensation. Nature. 2013; 493:221–225. [PubMed: 23222543]

Zhao Q, Wu K, Geng J, Chi S, Wang Y, Zhi P, Zhang M, Xiao B. Ion Permeation and Mechanotransduction Mechanisms of Mechanosensitive Piezo Channels. Neuron. 2016; 89:1248–1263. [PubMed: 26924440]

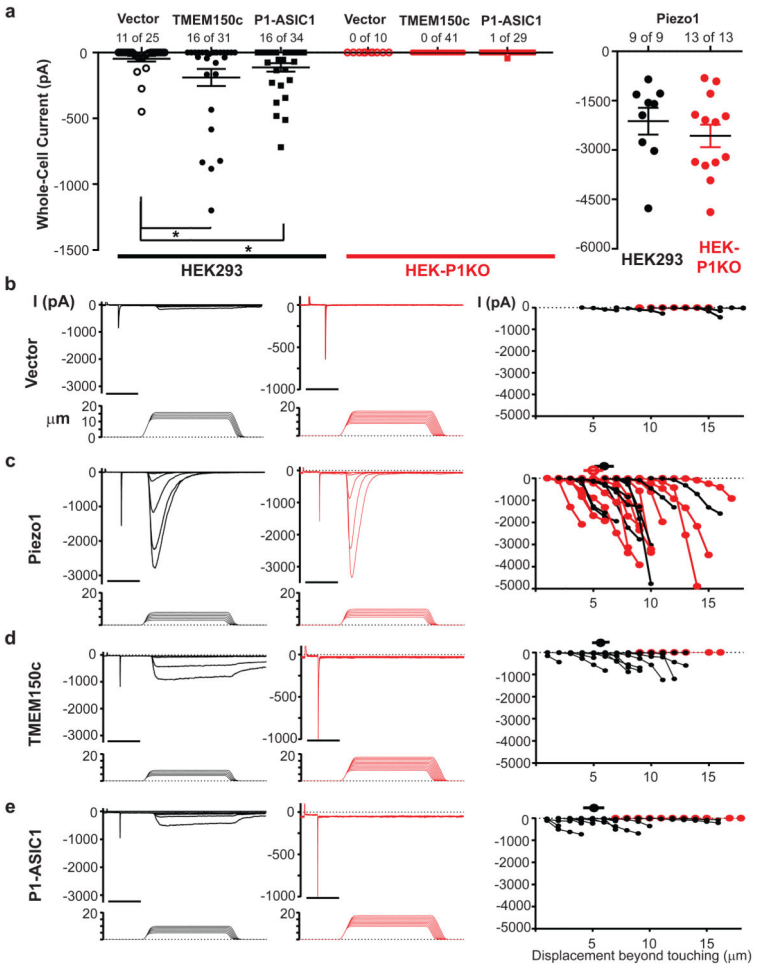

Figure 1.

Whole-cell MA currents in HEK cells transfected with vector, TMEM150c or Piezo1-ASIC1 ("P1-ASIC1") chimera are dependent on endogenous Piezo1 (performed at The Scripps Research Institute). **a. Left**: Scatter dot plot of maximal whole-cell current observed for each cell tested including non-responsive HEK cells (the number of responsive cells of the total tested is shown above each set). Maximal MA currents observed in TMEM150c and Piezo1-ASIC1 responsive cells held at -80 mV were statistically different from vector-transfected control HEK cells (*, P<0.05, Student's *t*-test; non-responsive cells are not included in this analysis). **Right**: I_{max} observed for either mouse or human Piezo1-pIres2-EGFP in HEK (black) or HEK-P1KO (red). Note the 4-fold change in the y-axis. I_{max} was measured at similar displacements above apparent threshold (4.0 ± 0.6 µm and 4.5 ± 0.7 µm for HEK and HEK-P1KO, respectively). Data are represented as mean ± S.E.M.. **b-e (left and middle panels)**. Whole-cell MA currents elicited by the protocol shown below for representative HEK (**left**) and HEK-P1KO (**middle**) cells transfected with pIRES2-EGFP (**b**), hPiezo1-pIres2-EGFP (**c**), TMEM150c-Ires-AcGFP (**d**) and mP1-mASIC1- mRuby (C-terminal fusion). (**e**). All horizontal scale bars represent 50 ms. **Right**: stimulus-response curves for each cell tested (black: HEK; red: HEK-P1KO). Circles above the stimulus-response curves represent the mean of the apparent thresholds observed for responsive HEK (black) and

HEK-P1KO (red) cells with the bar indicating ± S.E.M. (**c,d,e**). n represent individual cells. For panel **c (right)** the circles above the axis represent n=9 and 13 for HEK (black) and HEK-P1KO (red); for panel **d (right)**, n=16 for HEK; for panel **e (right)** n=16 for HEK.

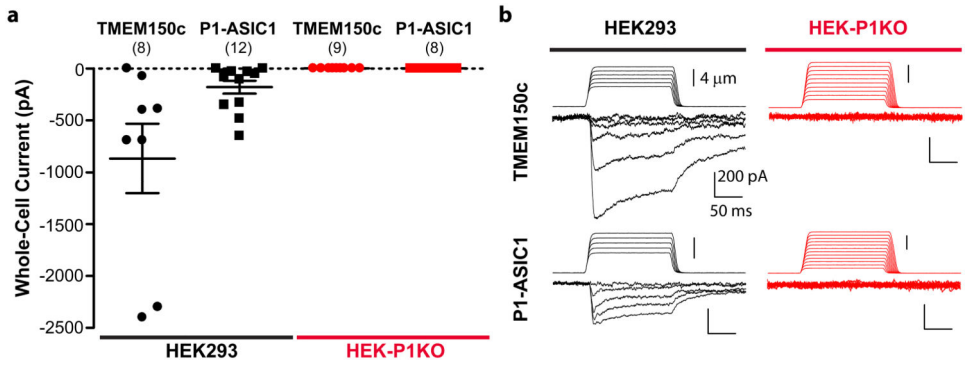

Figure 2.

Whole-cell MA currents in HEK cells transfected with TMEM150c or P1-ASIC1 chimera are dependent on endogenous Piezo1 (performed at Aix Marseille Universite). **a**. Scatter plot of I_{max} at -80 mV for each cell tested including non-responders. Mean ± S.E.M. is indicated for each set where applicable. **b**. Representative traces of MA currents recorded from TMEM150c (**top**)- and P1-ASIC1 (**bottom**)-transfected HEK (**left**, black traces) and HEK-P1KO (**right**, red traces) cells in response to the displacements shown above. Vertical scale bars: displacement, 4 µm; current, 200 pA. Horizontal scale bar: 50 ms.

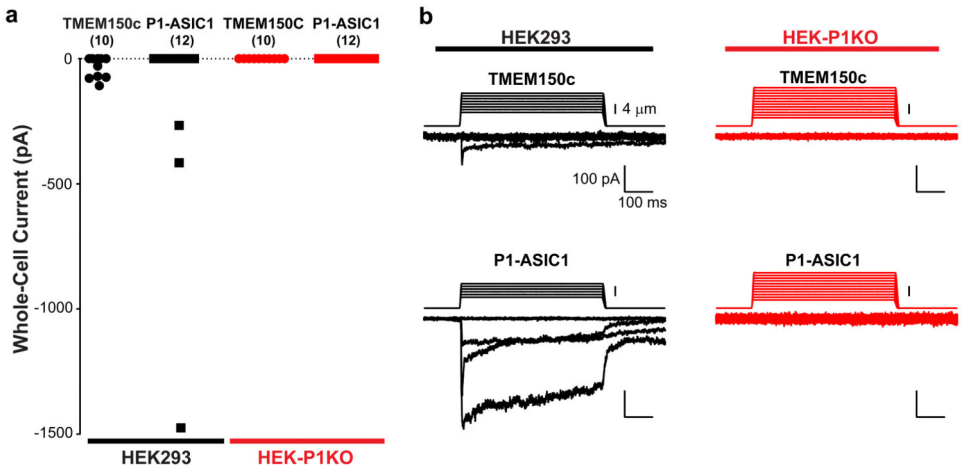

Figure 3.

Whole-cell MA currents in HEK cells transfected with TMEM150c or P1-ASIC1 chimera are dependent on endogenous Piezo1 (performed at Duke University). **a**. Scatter plot of Imax at -80 mV for each cell tested including non-responders. All cells in the dataset survived at least 7 µm past first touch. Mean ± S.E.M. is indicated for each set where applicable. **b**. Representative MA currents recorded from TMEM150c (**top**)- and P1-ASIC1 (**bottom**)-transfected HEK (**left**, black traces) and HEK-P1KO (**right**, red traces) cells in response to the displacements shown above. Vertical scale bars: displacement, 4 µm; current, 100 pA. Horizontal scale bar: 100 ms.

Table

Key Resources

REAGENT or RESOURCE	SOURCE	IDENTIFIER
Antibodies		
N/A		
Bacterial and Virus Strains		
N/A		
Biological Samples		
N/A		
Chemicals, Peptides, and Recombinant Proteins		
N/A		
Critical Commercial Assays		
N/A		
Deposited Data		
N/A		
Experimental Models: Cell Lines		
HEK293T	ATCC	CRL-3216
HEK293T	DSMZ	ACC-635
HEK-P1KO 5E3	This paper	N/A
HEK-P1KO 1C10	This paper	N/A
Experimental Models: Organisms/Strains		
N/A		
Oligonucleotides		
Primers hP1 Locus F: CCACGTGTAGGGTGACTGTT	This paper	N/A
Primers hP1 Locus R: GCCTCGTGATCAGCTAGTGG	This paper	N/A
Recombinant DNA		
mP1-mASIC1–mRuby (C-terminal fusion)	Zhao et al., 2016	N/A
TMEM150c-ires-AcGFP	Hong et al., 2016	N/A
hPiezo1-pIres2-EGFP	Lukacs et al., 2015	N/A
pIres2-EGFP empty vector	Lukacs et al., 2015	N/A
Software and Algorithms		
N/A		
Other		
N/A		